Mon. Not. R. Astron. Soc. **316**, 588–604 (2000)

Radiating gravitational collapse with shear viscosity

R. Chan★
[1]*Observatório Nacional, DAGE, Rua Gal. José Cristino 77, São Cristóvão, CEP 20921-400, Rio de Janeiro, Brazil*
[2]*University of Massachusetts, Department of Physics and Astronomy, Graduate Research Center, Amherst, MA 01003-4525, USA*

Accepted 2000 March 1. Received 2000 February 23; in original form 1999 September 30

ABSTRACT

A model is proposed of a collapsing radiating star consisting of an isotropic fluid with shear viscosity undergoing radial heat flow with outgoing radiation. The pressure of the star, at the beginning of the collapse, is isotropic but owing to the presence of the shear viscosity the pressure becomes more and more anisotropic. The behaviour of the density, pressure, mass, luminosity and the effective adiabatic index is analysed. Our work is compared to the case of a collapsing shearing fluid of a previous model, for a star with 6 $M_{\odot}$.

Key words: gravitation – relativity – supernovae: general.

1 INTRODUCTION

Many of the previous works in gravitational collapse have considered only shear-free motion of the fluid (de Oliveira, Santos & Kolassis 1985; Bonnor, de Oliveira & Santos 1989; Martínez & Pavón 1994). This simplification allows us to obtain exact solutions of the Einstein's equations in some cases but it is somewhat unrealistic. It is also unrealistic to consider heat flow without viscosity but if viscosity is introduced, it is desirable to allow shear in the fluid motion. Thus, it is interesting to study solutions that contain shear, because it plays a very important role in the study of gravitational collapse, as shown in Chan (1997, 1998). In that paper we compared two collapsing models: a shear-free and a shearing model. We were interested in studying the effect of the shear motion in the evolution of the collapse. It was shown that the pressure of the star, at the beginning of the collapse, is isotropic but owing to the presence of the shear the pressure becomes more and more anisotropic. The anisotropy in self-gravitating systems has been reviewed and the causes for its appearance discussed in Herrera & Santos (1997). As shown by Chan (1997, 1998) the simplest cause of the presence of anisotropy in a self-gravitating body is the shearing motion of the fluid, because it appears without an imposition ad hoc (Chan 1993).

The physical justification for this type of study is evident (Chan, Herrera & Santos 1994). Dissipative processes are not considered in most of the general relativistic calculations modelling gravitational collapses. This situation can be partially understood via the fact that, for highly condensed matter, with important general relativistic effects, the Fermi energy is much larger than the thermal energy. The collapsing configuration may then be considered to be essentially isentropic. This approximation is likely to fail in certain scenarios of the general relativistic stellar evolution. One example of such a situation is neutrino trapping, which is expected to occur during a gravitational collapse when the central density reaches values of the order of 10^{12} g cm^{-3} (Arnett 1977). Besides, the long mean free path and high energy density of these trapped neutrinos causes the viscosity in the fluid cores (Kazanas 1978).

The aim of this work is to generalize our previous model by introducing shear viscosity, besides the shear motion of the fluid, and compare it to the non-viscous collapse.

This work is organized as follows. In Section 2 we present Einstein's field equations. In Section 3 we re-derive the junction conditions, since Chan (1997, 1998) have obtained only results without shear viscosity. In Section 4 we present the proposed solution of the field equations. In Section 5 we describe the model considered in this work for the initial configuration. In Section 6 we present the energy conditions for a viscous anisotropic fluid. In Section 7 we show the time evolution of the total mass, luminosity and the effective adiabatic index and in Section 8 we summarize the main results obtained in this work.

2 FIELD EQUATIONS

We assume a spherically symmetric distribution of fluid undergoing dissipation in the form of heat flow. While the dissipative fluid collapses it produces radiation. The interior space–time is described by the most general spherically symmetric metric, using comoving

★ E-mail: chan@hobby.astro.umass.edu

coordinates,

$$ds_-^2 = -A^2(r,t)\,dt^2 + B^2(r,t)\,dr^2 + C^2(r,t)(d\theta^2 + \sin^2\theta\,d\phi^2). \tag{1}$$

The exterior space–time is described by Vaidya's (1953) metric, which represents an outgoing radial flux of radiation,

$$ds_+^2 = -\left[1 - \frac{2m(v)}{\boldsymbol{r}}\right]dv^2 - 2\,dv\,d\boldsymbol{r} + \boldsymbol{r}^2(d\theta^2 + \sin^2\theta\,d\phi^2), \tag{2}$$

where $m(v)$ represents the mass of the system inside the boundary surface Σ, function of the retarded time v.

We assume the interior energy–momentum tensor is given by

$$G_{\alpha\beta} = \kappa T_{\alpha\beta} = \kappa[(\mu + p_t)u_\alpha u_\beta + p_t g_{\alpha\beta} + (p - p_t)X_\alpha X_\beta + q_\alpha u_\beta + q_\beta u_\alpha - 2\eta\sigma_{\alpha\beta}], \tag{3}$$

where μ is the energy density of the fluid, p is the radial pressure, p_t is the tangential pressure, q^α is the radial heat flux, X_α is an unit four-vector along the radial direction, u^α is the four-velocity, which have to satisfy $u^\alpha q_\alpha = 0$, $X_\alpha X^\alpha = 1$, $X_\alpha u^\alpha = 0$ and $\kappa = 8\pi$ (i.e., $c = G = 1$). The quantity $\eta > 0$ is the coefficient of shearing viscosity and the shearing tensor $\sigma_{\alpha\beta}$ is defined as

$$\sigma_{\alpha\beta} = u_{(\alpha;\beta)} + \dot{u}_{(\alpha}u_{\beta)} - \tfrac{1}{3}\Theta(g_{\alpha\beta} + u_\alpha u_\beta), \tag{4}$$

with

$$\dot{u}_\alpha = u_{\alpha;\beta}u^\beta, \tag{5}$$

$$\Theta = u^\alpha_{;\alpha}, \tag{6}$$

where the semicolon denotes a covariant derivative and the parentheses in the indices mean symmetrizations. Here, we correct some misprints in equation (36) of Chan (1997). The correct equation for $\sigma_{\alpha\beta}$ is given here by equation (4).

Since we utilize comoving coordinates we have,

$$u^\alpha = A^{-1}\delta_0^\alpha, \tag{7}$$

and since the heat flux is radial

$$q^\alpha = q\delta_1^\alpha. \tag{8}$$

Thus the non-zero components of the shearing tensor are given by

$$\sigma_{11} = \frac{2B^2}{3A}\left(\frac{\dot{B}}{B} - \frac{\dot{C}}{C}\right), \tag{9}$$

$$\sigma_{22} = -\frac{C^2}{3A}\left(\frac{\dot{B}}{B} - \frac{\dot{C}}{C}\right), \tag{10}$$

$$\sigma_{33} = \sigma_{22}\sin^2\theta. \tag{11}$$

A simple calculation shows that

$$\sigma_{\alpha\beta}\sigma^{\alpha\beta} = \frac{2}{3A^2}\left(\frac{\dot{B}}{B} - \frac{\dot{C}}{C}\right)^2. \tag{12}$$

Thus, if we define the scalar σ as

$$\sigma = -\frac{1}{3A}\left(\frac{\dot{B}}{B} - \frac{\dot{C}}{C}\right), \tag{13}$$

we can write that

$$\sigma_{11} = -2B^2\sigma, \tag{14}$$

$$\sigma_{22} = C^2\sigma, \tag{15}$$

$$\sigma_{33} = C^2\sigma\sin^2\theta. \tag{16}$$

The non-vanishing components of the field equations, using (1), (3), (7), (8) and (14)–(16), interior of the boundary surface Σ are

$$G_{00}^- = -\left(\frac{A}{B}\right)^2\left[2\frac{C''}{C} + \left(\frac{C'}{C}\right)^2 - 2\frac{C'}{C}\frac{B'}{B}\right] + \left(\frac{A}{C}\right)^2 + \frac{\dot{C}}{C}\left(\frac{\dot{C}}{C} + 2\frac{\dot{B}}{B}\right) = \kappa A^2\mu, \tag{17}$$

$$G_{11}^- = \frac{C'}{C}\left(\frac{C'}{C} + 2\frac{A'}{A}\right) - \left(\frac{B}{C}\right)^2 - \left(\frac{B}{A}\right)^2\left[2\frac{\ddot{C}}{C} + \left(\frac{\dot{C}}{C}\right)^2 - 2\frac{\dot{A}}{A}\frac{\dot{C}}{C}\right] = \kappa B^2(p + 4\eta\sigma), \tag{18}$$

$$G_{22}^{-}=\left(\frac{C}{B}\right)^2\left[\frac{C''}{C}+\frac{A''}{A}+\frac{C'}{C}\frac{A'}{A}-\frac{A'}{A}\frac{B'}{B}-\frac{B'}{B}\frac{C'}{C}\right]+\left(\frac{C}{A}\right)^2\left[-\frac{\ddot{B}}{B}-\frac{\ddot{C}}{C}-\frac{\dot{C}}{C}\frac{\dot{B}}{B}+\frac{\dot{A}}{A}\frac{\dot{C}}{C}+\frac{\dot{A}}{A}\frac{\dot{B}}{B}\right]=\kappa C^2(p_t-2\eta\sigma), \tag{19}$$

$$G_{33}^{-}=G_{22}^{-}\sin^2\theta, \tag{20}$$

$$G_{01}^{-}=-2\frac{\dot{C}'}{C}+2\frac{C'}{C}\frac{\dot{B}}{B}+2\frac{A'}{A}\frac{\dot{C}}{C}=-\kappa AB^2q. \tag{21}$$

The dot and the prime stand for differentiation with respect to t and r, respectively.

3 JUNCTION CONDITIONS

We consider a spherical surface with its motion described by a time-like three-space Σ, which divides space–times into interior and exterior manifolds. For the junction conditions we follow the approach given by Israel (1966a,b). Hence we have to demand

$$(\mathrm{d}s_-^2)_\Sigma=(\mathrm{d}s_+^2)_\Sigma, \tag{22}$$

$$K_{ij}^{-}=K_{ij}^{+}, \tag{23}$$

where $K_{ij}^{\pm}$ is the extrinsic curvature to Σ, given by

$$K_{ij}^{\pm}=-n_\alpha^{\pm}\frac{\partial^2x^\alpha}{\partial\xi^i\partial\xi^j}-n_\alpha^{\pm}\Gamma^\alpha_{\beta\gamma}\frac{\partial x^\beta}{\partial\xi^i}\frac{\partial x^\gamma}{\partial\xi^j}, \tag{24}$$

and where $\Gamma^\alpha_{\beta\gamma}$ are the Christoffel symbols, $n_\alpha^{\mp}$ the unit normal vectors to Σ, x^α are the coordinates of interior and exterior space–times and ξ^i are the coordinates that define the surface Σ.

From the junction condition (22) we obtain

$$\frac{\mathrm{d}t}{\mathrm{d}\tau}=A(r_\Sigma,t)^{-1}, \tag{25}$$

$$C(r_\Sigma,t)=\boldsymbol{r}_\Sigma(v), \tag{26}$$

$$\left(\frac{\mathrm{d}v}{\mathrm{d}\tau}\right)_\Sigma^{-2}=\left(1-\frac{2m}{\boldsymbol{r}}+2\frac{\mathrm{d}\boldsymbol{r}}{\mathrm{d}v}\right)_\Sigma, \tag{27}$$

where τ is a time coordinate defined only on Σ.

The unit normal vectors to Σ (for details see Santos 1985) are given by

$$n_\alpha^{-}=B(r_\Sigma,t)\delta_\alpha^1, \tag{28}$$

$$n_\alpha^{+}=\left(1-\frac{2m}{\boldsymbol{r}}+2\frac{\mathrm{d}\boldsymbol{r}}{\mathrm{d}v}\right)_\Sigma^{-1/2}\left(-\frac{\mathrm{d}\boldsymbol{r}}{\mathrm{d}v}\delta_\alpha^0+\delta_\alpha^1\right)_\Sigma. \tag{29}$$

The non-vanishing extrinsic curvature are given by

$$K_{\tau\tau}^{-}=-\left[\left(\frac{\mathrm{d}t}{\mathrm{d}\tau}\right)^2\frac{A'A}{B}\right]_\Sigma, \tag{30}$$

$$K_{\theta\theta}^{-}=\left(\frac{C'C}{B}\right)_\Sigma, \tag{31}$$

$$K_{\phi\phi}^{-}=K_{\theta\theta}^{-}\sin^2\theta, \tag{32}$$

$$K_{\tau\tau}^{+}=\left[\frac{\mathrm{d}^2v}{\mathrm{d}\tau^2}\left(\frac{\mathrm{d}v}{\mathrm{d}\tau}\right)^{-1}-\left(\frac{\mathrm{d}v}{\mathrm{d}\tau}\right)\frac{m}{\boldsymbol{r}^2}\right]_\Sigma, \tag{33}$$

$$K_{\theta\theta}^{+}=\left[\left(\frac{\mathrm{d}v}{\mathrm{d}\tau}\right)\left(1-\frac{2m}{\boldsymbol{r}}\right)\boldsymbol{r}+\frac{\mathrm{d}\boldsymbol{r}}{\mathrm{d}\tau}\boldsymbol{r}\right]_\Sigma, \tag{34}$$

$$K_{\phi\phi}^{+}=K_{\theta\theta}^{+}\sin^2\theta. \tag{35}$$

From the equations (31) and (34) we have

$$\left[\left(\frac{\mathrm{d}v}{\mathrm{d}\tau}\right)\left(1-\frac{2m}{\boldsymbol{r}}\right)\boldsymbol{r}+\frac{\mathrm{d}\boldsymbol{r}}{\mathrm{d}\tau}\boldsymbol{r}\right]_\Sigma=\left(\frac{C'C}{B}\right)_\Sigma. \tag{36}$$

With the help of equations (25), (26) and (27), we can write (36) as

$$m = \left\{ \frac{C}{2} \left[1 + \left(\frac{\dot{C}}{A}\right)^2 - \left(\frac{C'}{B}\right)^2 \right] \right\}_\Sigma, \tag{37}$$

which is the total energy entrapped inside the surface Σ (Cahill & Mcvittie 1970).

From the equations (30) and (33), using (25), we have

$$\left[\frac{d^2 v}{d\tau^2} \left(\frac{dv}{d\tau}\right)^{-1} - \left(\frac{dv}{d\tau}\right) \frac{m}{\boldsymbol{r}^2} \right]_\Sigma = -\left(\frac{A'}{AB}\right)_\Sigma. \tag{38}$$

Substituting equations (25), (26) and (37) into (36) we can write

$$\left(\frac{dv}{d\tau}\right)_\Sigma = \left(\frac{C'}{B} + \frac{\dot{C}}{A}\right)^{-1}_\Sigma. \tag{39}$$

Differentiating (39) with respect to τ and using equations (37) and (39), we can rewrite (38) as

$$\left(\frac{C}{2AB}\right)_\Sigma \left\{ 2\frac{C'}{C} - 2\frac{C'}{C}\frac{\dot{B}}{B} - 2\frac{A'}{A}\frac{\dot{C}}{C} + \left(\frac{B}{A}\right)\left[2\frac{\ddot{C}}{C} - 2\frac{\dot{C}}{C}\frac{\dot{A}}{A} + \left(\frac{A}{C}\right)^2 + \left(\frac{\dot{C}}{C}\right)^2 - \left(\frac{A}{B}\right)^2 \left(\frac{C'}{C}\right)^2 - \left(\frac{A}{B}\right)^2 \left(2\frac{A'}{A}\frac{C'}{C}\right) \right] \right\}_\Sigma = 0. \tag{40}$$

Comparing (40) with (18) and (21), we can finally write

$$(p + 4\eta\sigma)_\Sigma = (qB)_\Sigma. \tag{41}$$

This result is analogous to the one obtained by Chan (1997, 1998) for a shearing fluid motion but now we have generalized for an interior fluid with shear viscosity.

The total luminosity for an observer at rest at infinity is

$$L_\infty = -\left(\frac{dm}{dv}\right)_\Sigma = -\left[\frac{dm}{dt}\frac{dt}{d\tau}\left(\frac{dv}{d\tau}\right)^{-1} \right]_\Sigma. \tag{42}$$

Differentiating (37) with respect to t, using (25), (39) and (18), we obtain that

$$L_\infty = \frac{\kappa}{2}\left[(p + 4\eta\sigma) C^2 \left(\frac{C'}{B} + \frac{\dot{C}}{A}\right)^2 \right]_\Sigma. \tag{43}$$

The boundary redshift can be used to determine the time of formation of the horizon. The boundary redshift z_Σ is given by

$$\left(\frac{dv}{d\tau}\right)_\Sigma = 1 + z_\Sigma. \tag{44}$$

The redshift, for an observer at rest at infinity diverges at the time of formation of the black hole. From (39) we can see that this happens when

$$\left(\frac{C'}{B} + \frac{\dot{C}}{A}\right)_\Sigma = 0. \tag{45}$$

4 SOLUTION OF THE FIELD EQUATIONS

Again as in Chan (1997, 1998) we propose solutions of the field equations (17)–(21) with the form

$$A(r,t) = A_0(r), \tag{46}$$

$$B(r,t) = B_0(r), \tag{47}$$

$$C(r,t) = rB_0(r)f(t), \tag{48}$$

where $A_0(r)$ and $B_0(r)$ are solutions of a static perfect fluid having μ_0 as the energy density and p_0 as the isotropic pressure. We remark that, following the junction condition equation (26), the function $C(r_\Sigma, t)$ represents the luminosity radius of the body as seen by an exterior observer.

Thus, the shear scalar (13) can be written as

$$\sigma = \frac{1}{3A_0}\frac{\dot{f}}{f}. \tag{49}$$

Now the equations (17)–(21) can be written as

$$\kappa\mu = \kappa\mu_0 + \frac{1}{A_0^2}\left(\frac{\dot{f}}{f}\right)^2 + \frac{1}{r^2B_0^2}\left(\frac{1}{f^2} - 1\right), \tag{50}$$

$$\kappa p = \kappa p_0 - \frac{1}{A_0^2}\left[2\frac{\ddot{f}}{f} + \left(\frac{\dot{f}}{f}\right)^2\right] - \frac{1}{r^2B_0^2}\left(\frac{1}{f^2} - 1\right) - \frac{4\kappa\eta}{3A_0}\frac{\dot{f}}{f}, \tag{51}$$

$$\kappa p_t = \kappa p_0 - \frac{1}{A_0^2}\frac{\ddot{f}}{f} + \frac{2\kappa\eta}{3A_0}\frac{\dot{f}}{f}, \tag{52}$$

$$\kappa q = \frac{2}{A_0B_0^2}\left(\frac{\dot{f}}{f}\right)\left(\frac{B_0'}{B_0} + \frac{1}{r} - \frac{A_0'}{A_0}\right), \tag{53}$$

where

$$\kappa\mu_0 = -\frac{1}{B_0^2}\left[2\frac{B_0''}{B_0} - \left(\frac{B_0'}{B_0}\right)^2 + \frac{4}{r}\frac{B_0'}{B_0}\right], \tag{54}$$

$$\kappa p_0 = \frac{1}{B_0^2}\left[\left(\frac{B_0'}{B_0}\right)^2 + \frac{2}{r}\frac{B_0'}{B_0} + 2\frac{A_0'}{A_0}\frac{B_0'}{B_0} + \frac{2}{r}\frac{A_0'}{A_0}\right]. \tag{55}$$

We can see from equations (50)–(53) that when the function $f(t) = 1$ we obtain the static perfect fluid configuration.

Substituting equations (51), (53) and (49) into (41), assuming also that $p_0(r_\Sigma) = 0$, we obtain a second-order differential equation in $f(t)$,

$$2f\ddot{f} + \dot{f}^2 + af\dot{f} + b(1 - f^2) = 0, \tag{56}$$

where

$$a = \left[2\left(\frac{A_0}{B_0}\right)\left(\frac{B_0'}{B_0} + \frac{1}{r} - \frac{A_0'}{A_0}\right)\right]_\Sigma, \tag{57}$$

and

$$b = \left(\frac{A_0^2}{r^2B_0^2}\right)_\Sigma. \tag{58}$$

This equation is identical to the one obtained in Chan (1997, 1998). Thus, as before it has to be solved numerically (Fig. 1), assuming that at $t \to -\infty$ represents the static configuration with $\dot{f}(t \to -\infty) \to 0$ and $f(t \to -\infty) \to 1$. We also assume that $f(t \to 0) \to 0$. This means that the luminosity radius $C(r_\Sigma, t)$ has the value $r_\Sigma B_0(r_\Sigma)$ at the beginning of the collapse and vanishing at the end of the evolution.

5 MODEL OF THE INITIAL CONFIGURATION

We consider that the system at the beginning of the collapse has a static configuration of a perfect fluid satisfying the Schwarzschild interior solution (Raychaudhuri & Maiti 1979)

$$A_0 = \frac{g(r)}{2(1 + r_\Sigma^2)(1 + r^2)}, \tag{59}$$

$$B_0 = \frac{2R}{1 + r^2}, \tag{60}$$

where

$$g(r) = 3(1 - r_\Sigma^2)(1 + r^2) - (1 + r_\Sigma^2)(1 - r^2), \tag{61}$$

and

$$R = m_0\frac{(1 + r_\Sigma^2)^3}{4r_\Sigma^3}. \tag{62}$$

and where r_Σ is the initial radius of the star in comoving coordinates and m_0 is the initial mass of the system. Thus the static uniform energy density and static pressure are given by

$$\kappa\mu_0 = \frac{3}{R^2}, \tag{63}$$

$$\kappa p_0 = \frac{6}{R^2}\frac{(r_\Sigma^2 - r^2)}{g(r)}. \tag{64}$$

We consider the initial configuration as owing to a helium core of a pre-supernova with $m_0 = 6\,M_\odot$, initial radius $r_\Sigma = 1.6 \times 10^5$ km

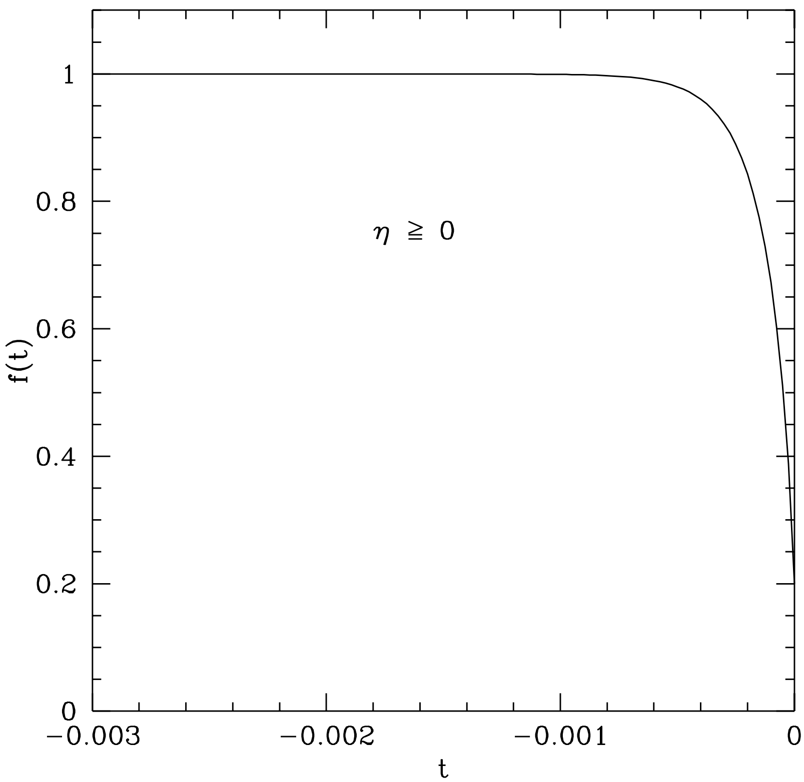

Figure 1. Time behaviour of the function $f(t)$ for the models with and without shear viscosity. The time is in units of seconds and $f(t)$ is dimensionless.

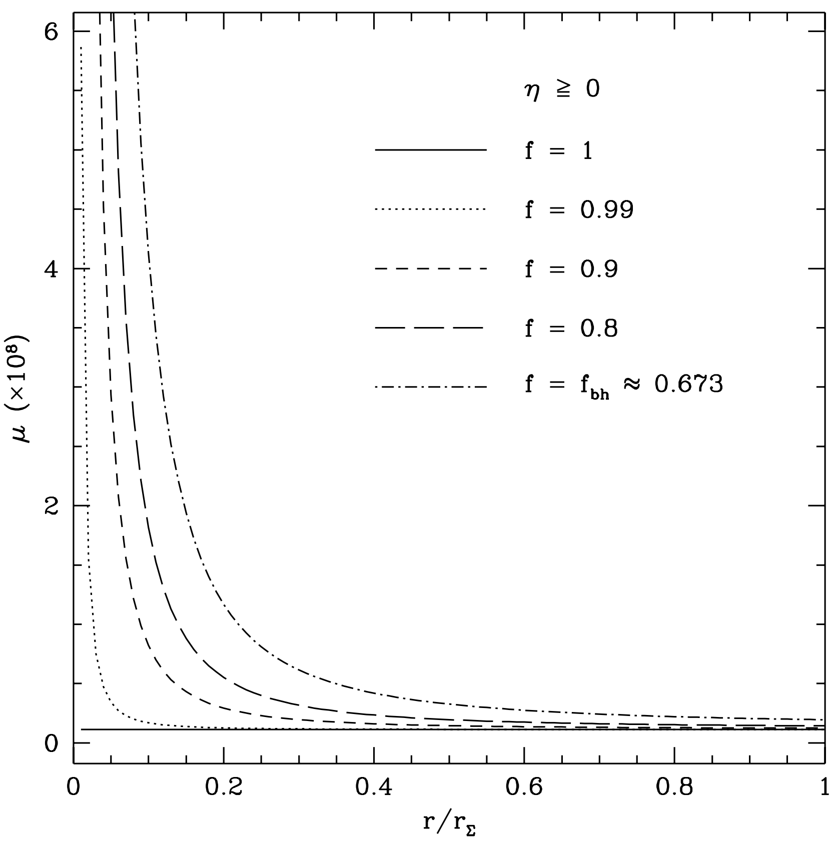

Figure 2. Density profiles for the model with and without shear viscosity. The radii r and r_Σ are in units of seconds and the density is in units of s^{-2}.

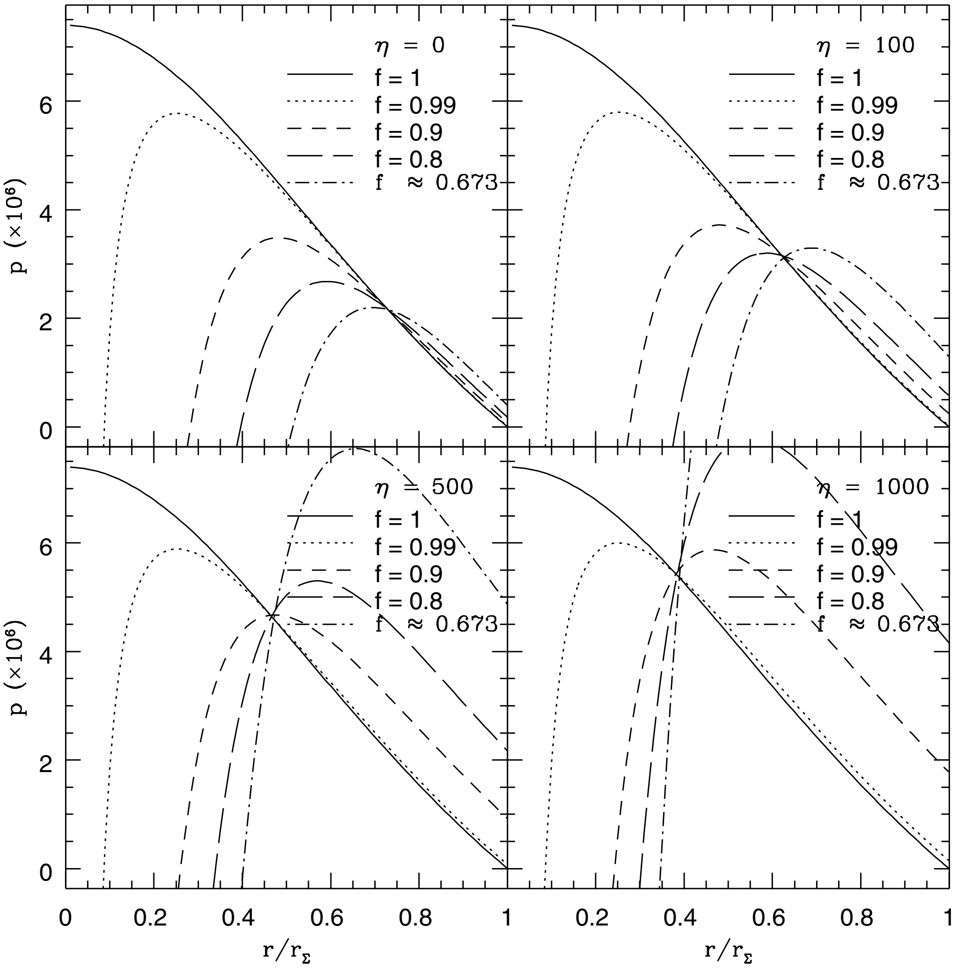

Figure 3. Radial pressure profiles for four different values of η. The radii r and r_Σ are in units of seconds and the radial pressure is in units of s^{-2}.

(Woosley & Phillips 1988). With these values we can solve numerically the differential equation (56). We can see from equation (53), using (59)–(62) and this initial configuration, that $[(B_0'/B_0 + 1/r - A_0'/A_0)/A_0]_\Sigma < 0$ and by the fact that $q_\Sigma > 0$ we then conclude that $\dot{f} < 0$.

In order to determine the time of formation of the horizon $f_{\rm bh}$, we use the equations (37), (45) and (46)–(48) and write

$$\frac{\dot{f}_{\rm bh}}{f_{\rm bh}} = -\left[\frac{A_0}{B_0}\left(\frac{B_0'}{B_0} + \frac{1}{r}\right)\right]_\Sigma \approx -3.606 \times 10^3, \tag{65}$$

which gives us $f_{\rm bh} \approx 0.673$ ($t \approx -1.275 \times 10^{-4}$), using the numerical solution of $f(t)$.

We will assume that η is constant, but in general the shear viscosity coefficient depends on the temperature and density of the fluid (Cutler & Lindblom 1987). Hereinafter, the values of η will be 1.347×10^{30}, 6.736×10^{30} and 1.347×10^{31} g cm^{-1} s^{-1}, which correspond to values 100, 500 and 1000 s^{-1}, respectively, in time units.

In Fig. 2 we show the time evolution of the density profiles for the model with and without shear viscosity.

In Fig. 3 we notice that the radial pressure increases with the shear viscosity while the tangential pressure (Fig. 4) diminishes with the viscosity.

In Fig. 6 we show the time evolution of the heat flux scalar profiles for the model with and without shear viscosity.

In Fig. 5 ($\eta = 0$) we can see that the star is isotropic at the beginning of the collapse ($f = 1$) but becoming more and more anisotropic at later times. The anisotropy for the viscous model ($\eta \neq 0$) has the same time behaviour.

6 ENERGY CONDITIONS FOR A VISCOUS ANISOTROPIC FLUID

Following the same procedure used in Kolassis, Santos & Tsoubelis (1988) we can generalize the energy conditions for a viscous anisotropic fluid.

For the energy-momentum tensor Segre type [111,1] and if λ_0 denotes the eigenvalue corresponding to the time-like eigenvector, the general energy conditions are equivalent to the following relations between the eigenvalues of the energy–momentum tensor:

(a) weak energy condition

$$-\lambda_0 \geqslant 0, \tag{66}$$

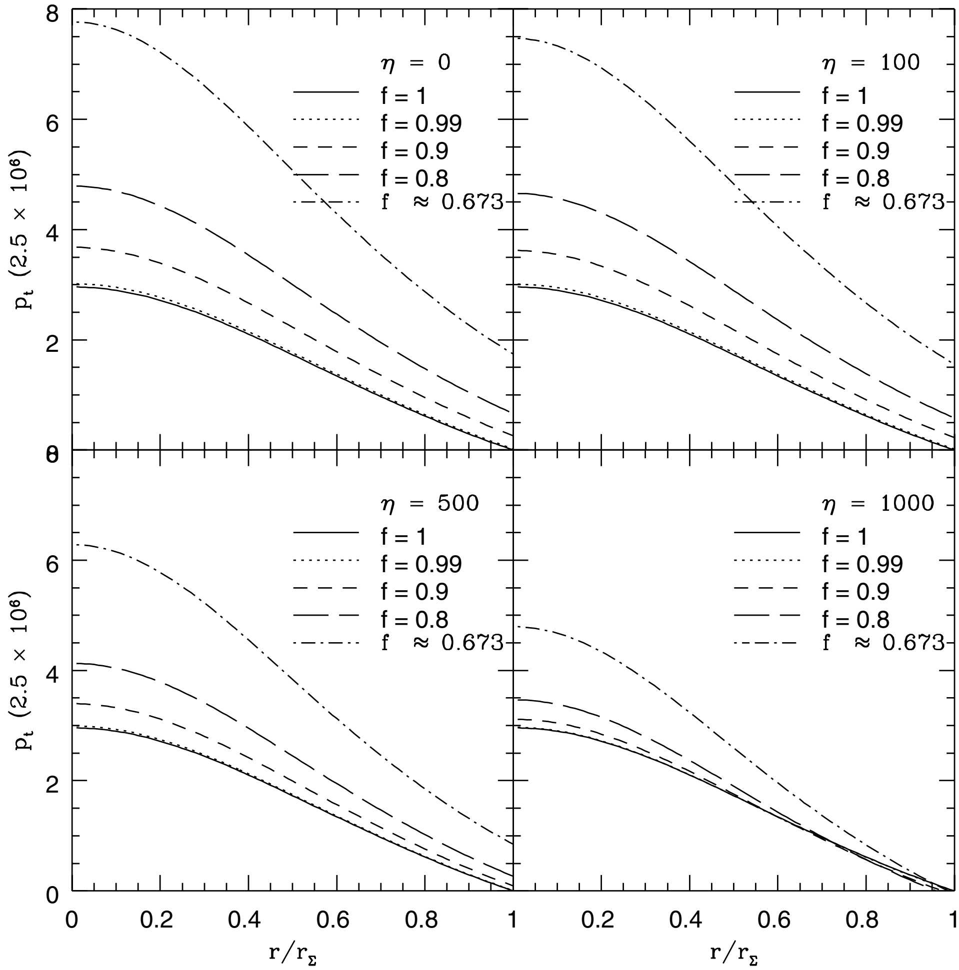

Figure 4. Tangential pressure profiles for four different values of η. The radii r and r_Σ are in units of seconds and the tangential pressure p_t is in units of s^{-2}.

and

$$-\lambda_0 + \lambda_i \geqslant 0, \tag{67}$$

(b) dominant energy condition

$$\lambda_0 \leqslant \lambda_i \leqslant -\lambda_0, \tag{68}$$

(c) strong energy condition

$$-\lambda_0 + \sum_i \lambda_i \geqslant 0, \tag{69}$$

and

$$-\lambda_0 + \lambda_i \geqslant 0, \tag{70}$$

where the values $i = 1, 2, 3$ represent the eigenvalues corresponding to the space-like eigenvectors.

The eigenvalues λ of the energy–momentum tensor are the roots of the equation

$$|T_{\alpha\beta} - \lambda g_{\alpha\beta}| = 0. \tag{71}$$

Since λ is a scalar we can use a locally Minkowskian coordinate system, we have

$$u^\alpha = \delta_0^\alpha, \tag{72}$$

$$X^\alpha = \delta_1^\alpha, \tag{73}$$

$$q^\alpha = q\delta_1^\alpha. \tag{74}$$

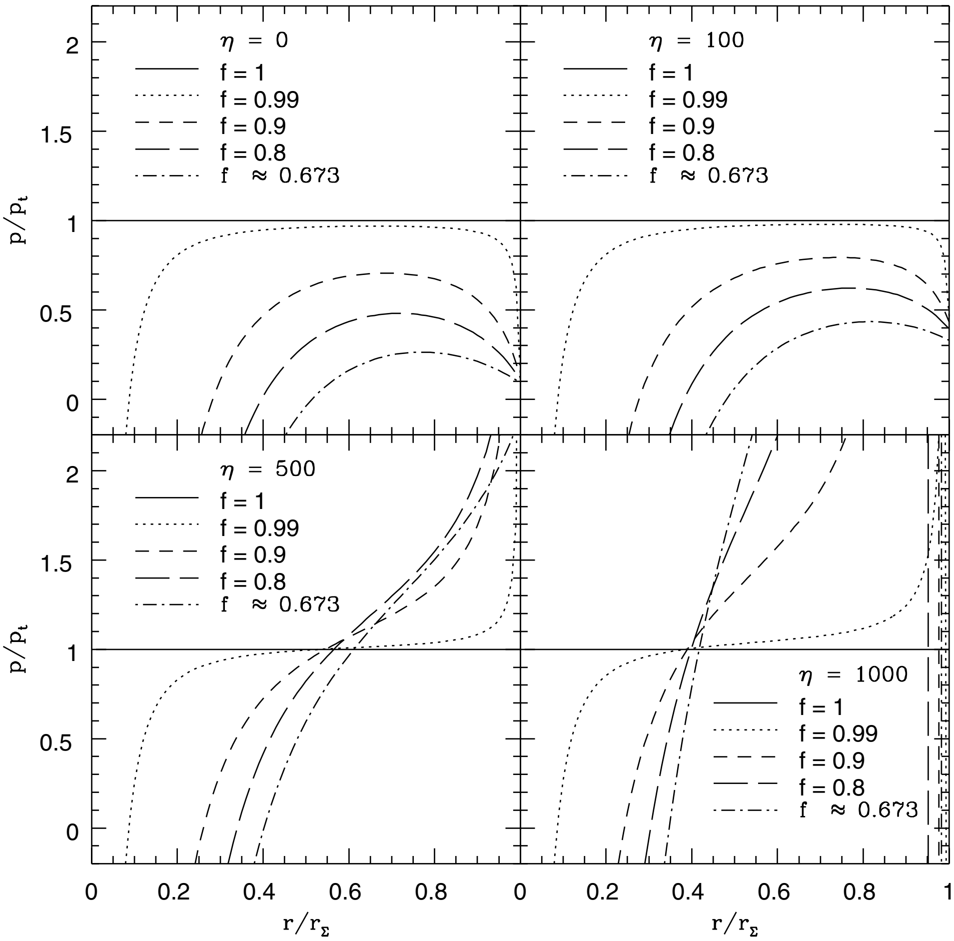

Figure 5. The profiles for four different values of η of the ratio between the radial and tangential pressures. The radii r and r_Σ are in units of seconds; and the radial and tangential pressure,p and p_t, are in units of s^{-2}.

Thus, we can rewrite equation (71) as

$$\begin{vmatrix} \mu+\lambda & -q & 0 & 0 \\ -q & p-\lambda-2\eta\sigma_{11} & 0 & 0 \\ 0 & 0 & p_t-\lambda-2\eta\sigma_{22} & 0 \\ 0 & 0 & 0 & p_t-\lambda-2\eta\sigma_{33} \end{vmatrix} = 0,$$

where the determinant of this equation is given by

$$[(\mu+\lambda)(\lambda-p+2\eta\sigma_{11})+q^2](\lambda-p_t+2\eta\sigma_{22})(\lambda-p_t+2\eta\sigma_{33})=0. \tag{75}$$

Thus, one of the solutions of the equation (75) is

$$[(\mu+\lambda)(\lambda-p+2\eta\sigma_{11})+q^2]=0, \tag{76}$$

which can be rewritten as

$$\lambda^2+(\mu-p+2\eta\sigma_{11})\lambda+q^2-\mu(p-2\eta\sigma_{11})=0. \tag{77}$$

The two roots of the equation (77) are

$$\lambda_0=-\tfrac{1}{2}(\mu-p+2\eta\sigma_{11}+\Delta), \tag{78}$$

and

$$\lambda_1=-\tfrac{1}{2}(\mu-p+2\eta\sigma_{11}-\Delta), \tag{79}$$

where

$$\Delta^2 = (\mu + p - 2\eta\sigma_{11})^2 - 4q^2 \geqslant 0, \tag{80}$$

must be greater or equal to zero in order to have real solutions. This equation can be rewritten as

$$|\mu + p - 2\eta\sigma_{11}| - 2|q| \geqslant 0. \tag{81}$$

The second solution of the equation (75) is

$$(\lambda - p_t + 2\eta\sigma_{22})(\lambda - p_t + 2\eta\sigma_{33}) = 0, \tag{82}$$

whose roots are given by

$$\lambda_2 = p_t - 2\eta\sigma_{22}, \tag{83}$$

and

$$\lambda_3 = p_t - 2\eta\sigma_{33}. \tag{84}$$

6.1 Weak energy conditions

From equations (66) and (78) we get the first weak energy condition written as

$$\mu - p + 2\eta\sigma_{11} + \Delta \geqslant 0. \tag{85}$$

From equation (67), setting $i = 1$ and using equations (78) and (79) we get the second weak energy condition given by

$$\Delta \geqslant 0, \tag{86}$$

which is equal to the condition (80).

From equation (67), now setting $i = 2$ and using equations (78) and (83) we get the third weak energy condition given by

$$\mu - p + 2\eta\sigma_{11} + 2(p_t - 2\eta\sigma_{22}) + \Delta \geqslant 0. \tag{87}$$

From equation (67), now setting $i = 3$ and using equations (78) and (84) we get the fourth weak energy condition given by

$$\mu - p + 2\eta\sigma_{11} + 2(p_t - 2\eta\sigma_{33}) + \Delta \geqslant 0. \tag{88}$$

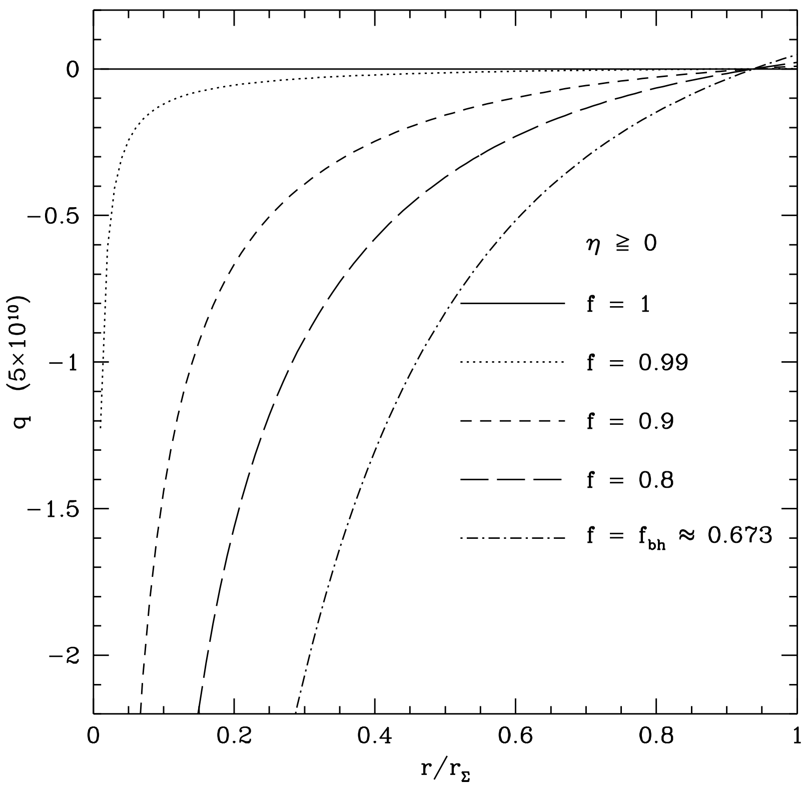

Figure 6. Heat flux scalar profiles for the model with and without shear viscosity. The radius r and r_Σ are in units of seconds and the heat flux q is in units of s^{-2}.

6.2 Dominant energy conditions

From equation (68), setting $i = 1$ and using equations (78) and (79) we obtain the inequality

$$-(\mu - p + 2\eta\sigma_{11} + \Delta) \leqslant -(\mu - p + 2\eta\sigma_{11} - \Delta) \leqslant \mu - p + 2\eta\sigma_{11} + \Delta, \tag{89}$$

which can be split into two inequalities, given by

$$\Delta \geqslant 0, \tag{90}$$

and

$$\mu - p + 2\eta\sigma_{11} \geqslant 0. \tag{91}$$

From equation (68), setting $i = 2$ and using equations (78) and (83) we get the inequality

$$-(\mu - p + 2\eta\sigma_{11} + \Delta) \leqslant 2(p_t - 2\eta\sigma_{22}) \leqslant \mu - p + 2\eta\sigma_{11} + \Delta, \tag{92}$$

which again we can split it into two inequalities, given by

$$\mu - p + 2\eta\sigma_{11} + 2(p_t - 2\eta\sigma_{22}) + \Delta \geqslant 0, \tag{93}$$

and

$$\mu - p + 2\eta\sigma_{11} - 2(p_t - 2\eta\sigma_{22}) + \Delta \geqslant 0. \tag{94}$$

From equation (68), setting $i = 3$ and using equations (78) and (84) we get the inequality

$$-(\mu - p + 2\eta\sigma_{11} + \Delta) \leqslant 2(p_t - 2\eta\sigma_{33}) \leqslant \mu - p + 2\eta\sigma_{11} + \Delta, \tag{95}$$

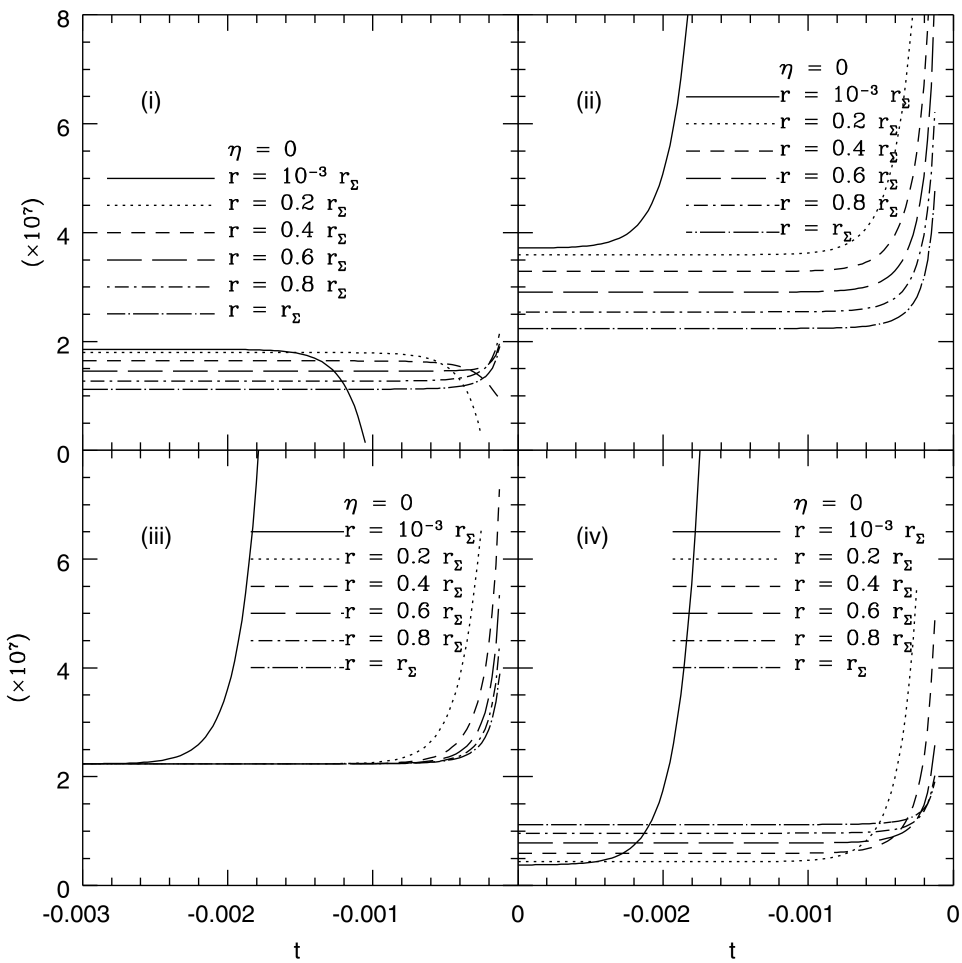

Figure 7. The energy conditions (110)–(113), for the model without shear viscosity, where $\eta = 0$. The time is in units of seconds and all the others quantities are in units of s^{-2}.

which again we can split it into two inequalities, given by

$$\mu - p + 2\eta\sigma_{11} + 2(p_t - 2\eta\sigma_{33}) + \Delta \geqslant 0, \tag{96}$$

and

$$\mu - p + 2\eta\sigma_{11} - 2(p_t - 2\eta\sigma_{33}) + \Delta \geqslant 0. \tag{97}$$

6.3 Strong energy conditions

Substituting equations (78), (79), (83) and (84) into equation (69) we get the first strong energy condition given by

$$2p_t - 2\eta(\sigma_{22} + \sigma_{33}) + \Delta \geqslant 0. \tag{98}$$

Since one of the weak energy conditions, equation (67), is the same for the strong energy condition (equation 70), thus we have that the second, third and fourth strong energy conditions are equal to equations (86)–(88), given by

$$\Delta \geqslant 0, \tag{99}$$

$$\mu - p + 2\eta\sigma_{11} + 2(p_t - 2\eta\sigma_{22}) + \Delta \geqslant 0, \tag{100}$$

and

$$\mu - p + 2\eta\sigma_{11} + 2(p_t - 2\eta\sigma_{33}) + \Delta \geqslant 0. \tag{101}$$

6.4 Summary of the energy conditions

Summarizing the results, we rewrite the energy conditions. The energy conditions for a spherically symmetric fluid whose energy–momentum

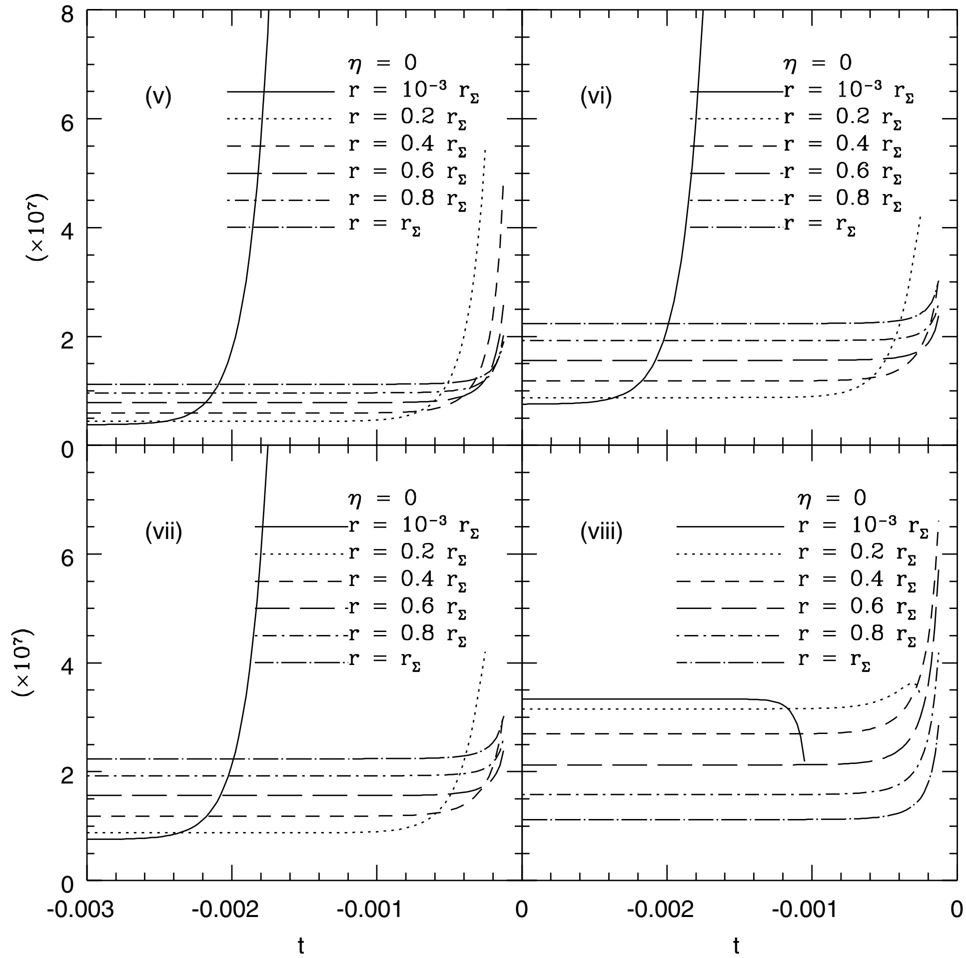

Figure 8. The energy conditions (114)–(117), for the model without shear viscosity, where $\eta = 0$. The time is in units of seconds and all the others quantities are in units of s^{-2}.

tensor is given by equation (3) are fulfilled if the following inequalities are satisfied:

(i) $|\mu + p - 2\eta\sigma_{11}| - 2|q| \geqslant 0,$ (102)

(ii) $\mu - p + 2p_t + \Delta + 2\eta(\sigma_{11} - 2\sigma_{22}) \geqslant 0,$ (103)

(iii) $\mu - p + 2p_t + \Delta + 2\eta(\sigma_{11} - 2\sigma_{33}) \geqslant 0,$ (104)

and besides,
(a) for the weak energy conditions

(iv) $\mu - p + \Delta + 2\eta\sigma_{11} \geqslant 0,$ (105)

(b) for the dominant energy conditions

(v) $\mu - p + 2\eta\sigma_{11} \geqslant 0,$ (106)

(vi) $\mu - p - 2p_t + \Delta + 2\eta(\sigma_{11} + 2\sigma_{22}) \geqslant 0,$ (107)

(vii) $\mu - p - 2p_t + \Delta + 2\eta(\sigma_{11} + 2\sigma_{33}) \geqslant 0,$ (108)

(c) for the strong energy conditions

(viii) $2p_t + \Delta - 2\eta(\sigma_{22} + \sigma_{33}) \geqslant 0,$ (109)

where $\Delta = \sqrt{(\mu + p - 2\eta\sigma_{11})^2 - 4q^2}$.

These equations, using equations (14)–(16) and (46)–(48), can be rewritten as

(i) $|\mu + p + 4\eta B_0^2\sigma| - 2|q| \geqslant 0,$ (110)

(ii) $\mu - p + 2p_t + \Delta - 4\eta B_0^2\sigma(1 + r^2f^2) \geqslant 0,$ (111)

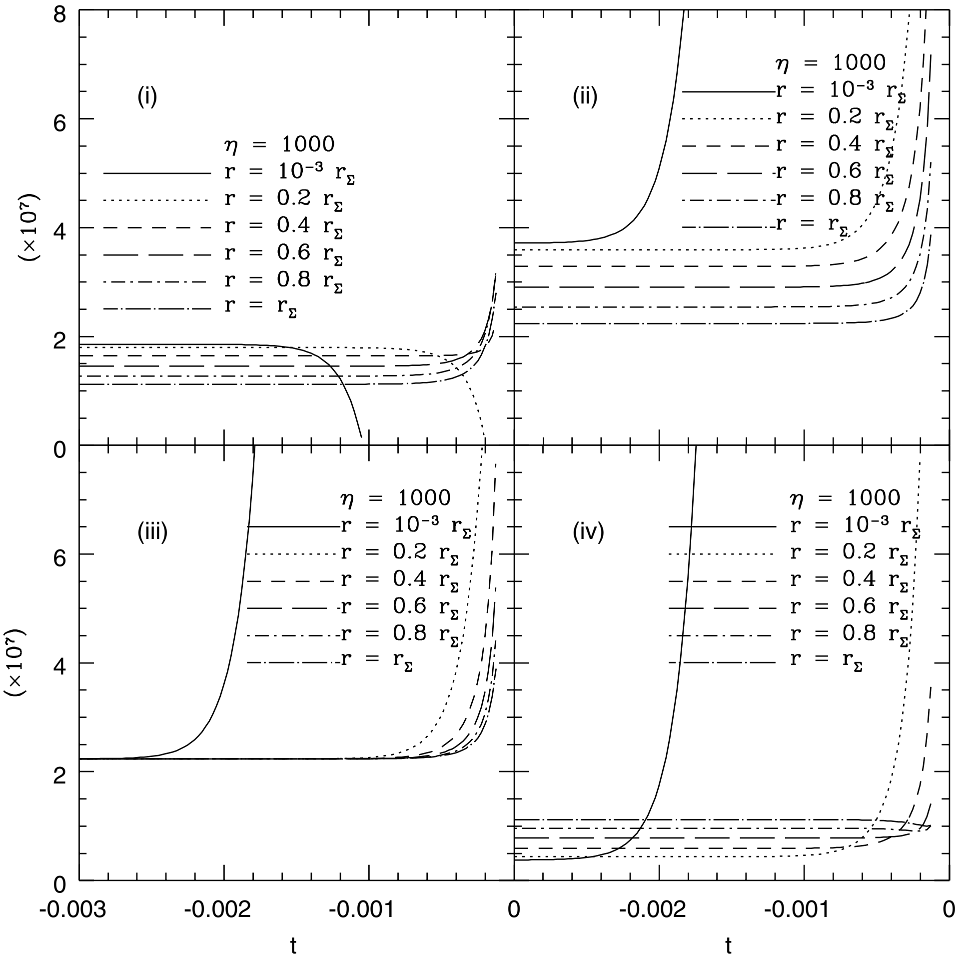

Figure 9. The energy conditions (110)–(113), for the model with shear viscosity, where $\eta = 1000$. The time is in units of seconds and all the others quantities are in units of s^{-2}.

(iii) $\mu - p + 2p_t + \Delta - 4\eta B_0^2\sigma(1 + r^2 f^2 \sin^2\theta) \geqslant 0,$ (112)

(iv) $\mu - p + \Delta - 4\eta B_0^2\sigma \geqslant 0,$ (113)

(v) $\mu - p - 4\eta B_0^2\sigma \geqslant 0,$ (114)

(vi) $\mu - p - 2p_t + \Delta - 4\eta B_0^2\sigma(1 - r^2 f^2) \geqslant 0,$ (115)

(vii) $\mu - p - 2p_t + \Delta - 4\eta B_0^2\sigma(1 - r^2 f^2 \sin^2\theta) \geqslant 0,$ (116)

(viii) $2p_t + \Delta - 2\eta r^2 B_0^2 \sigma f^2(1 + \sin^2\theta) \geqslant 0,$ (117)

where $\Delta = \sqrt{(\mu + p + 4\eta B_0^2\sigma)^2 - 4q^2}$. In order to minimize the values of the equations (112), (116) and (117) in relation to θ, we have chosen the values of $\sin^2\theta = 0, 1, 1$, respectively, since $\eta \geqslant 0$ and $\sigma \leqslant 0(\dot{f} \leqslant 0, A_0 > 0)$.

In order to verify the energy conditions, we have plotted the time evolution of all the conditions, for several radii and for two values of η (0 and 1000), as we can see in the Figs 7, 8, 9 and 10. For the sake of comparison with the model $\eta \neq 0$, we have plotted all the conditions (110)–(117) for $\eta = 0$, even though in this case some of them are identical.

From the Figs 7(i) and 9(i) we can conclude that only the inequality $[|\mu + p + 4\eta B_0^2\sigma| - 2|q| \geqslant 0]$ is not satisfied during all the collapse and for any radius. This inequality is not satisfied for the innermost radii ($r \leqslant 0.2r_\Sigma$) and for the latest stages of the collapse. The condition (117) is not satisfied for $r < 0.2r_\Sigma$ [Figs 8(viii) and 10(viii)] because the inequality (110) [$\Delta \geqslant 0$] is not satisfied for these radii and for the latest stages of the collapse.

7 PHYSICAL RESULTS

As in Chan (1997, 1998), we have calculated several physical quantities, as the total energy entrapped inside the Σ surface, the total

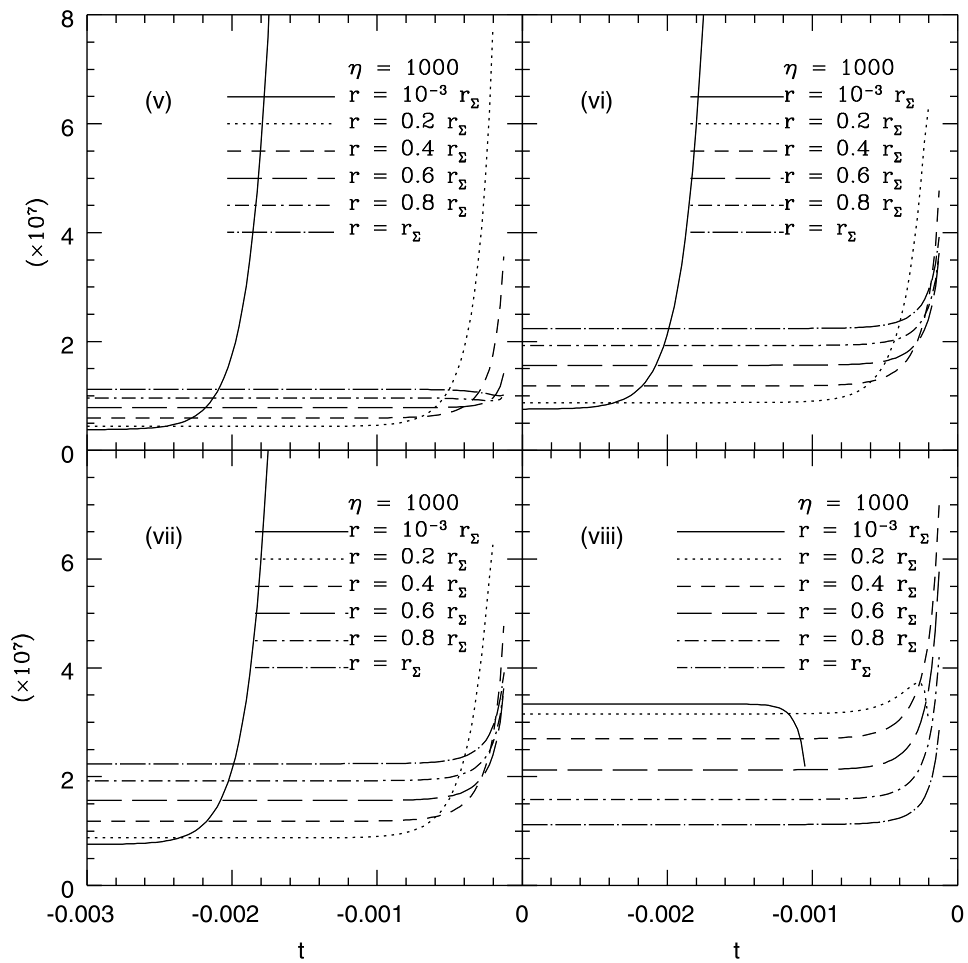

Figure 10. The energy conditions (114)–(117), for the model with shear viscosity, where $\eta = 1000$. The time is in units of seconds and all the others quantities are in units of s^{-2}.

luminosity perceived by an observer at rest at infinity and the effective adiabatic index, and we have compared them to the respective non-viscous ones.

From equation (37) we can write using (46)–(48) that

$$m = \left[\frac{r^3 B_0^3}{2A_0^2} f\dot{f}^2 + \frac{rB_0}{2} f(1-f^2) + m_0 f^3\right]_\Sigma, \tag{118}$$

where

$$m_0 = -\left[r^2 B'_0 + \frac{r^3 B'^2_0}{2B_0}\right]_\Sigma. \tag{119}$$

We can observe from Fig. 11 that the mass inside Σ is equal for both models, with and without shear viscosity. This means that they radiate the same amount of mass during the evolution.

Using the equations (43) and (46)–(48) we can write the luminosity of the star as

$$L_\infty = \frac{\kappa}{2}\left\{(p + 4\eta\sigma) r^2 B_0^2 f^2 \left[\left(r\frac{B'_0}{B_0} + 1\right) f + \left(\frac{rB_0}{A_0}\right)\dot{f}\right]^2\right\}_\Sigma. \tag{120}$$

This equation apparently depends on the viscosity but if we substitute the equations (49) and (51) into (120) the viscosity dependence vanishes remaining only the pressure without shear viscosity. That is the reason we have presented in Fig. 12 a single plot for both models.

The effective adiabatic index can be calculated using the equations (50), (51), (56) and (59)–(64). Thus, we can write that

$$\Gamma_{\rm eff} = \left[\frac{\partial(\ln p)}{\partial(\ln\mu)}\right]_{r=\rm constant} = \left(\frac{\dot{p}}{p}\right)\left(\frac{\mu}{\dot{\mu}}\right) = \frac{c(r)f[3j(r)\dot{f}^2 + bj(r)(1-f^2)] + \dot{f}\{c(r)[12b + aj(r)f^2] - 12d(r)]\}}{c(r)[6\dot{f}^3 + 2af\dot{f}^2] + \dot{f}[2c(r)b(1-f^2) + 4d(r)]}$$
$$\times \frac{12r^2 d(r) f^2 + h(r)[c(r)\dot{f}^2 + d(r)(1-f^2)]}{72r^2 e(r) f^2 + h(r)\{c(r)j(r)f\dot{f} + 3[bc(r) - d(r)](1-f^2)\}}, \tag{121}$$

where

$$c(r) = r^2 m_0^2 (1 + r_\Sigma^2)^8, \tag{122}$$

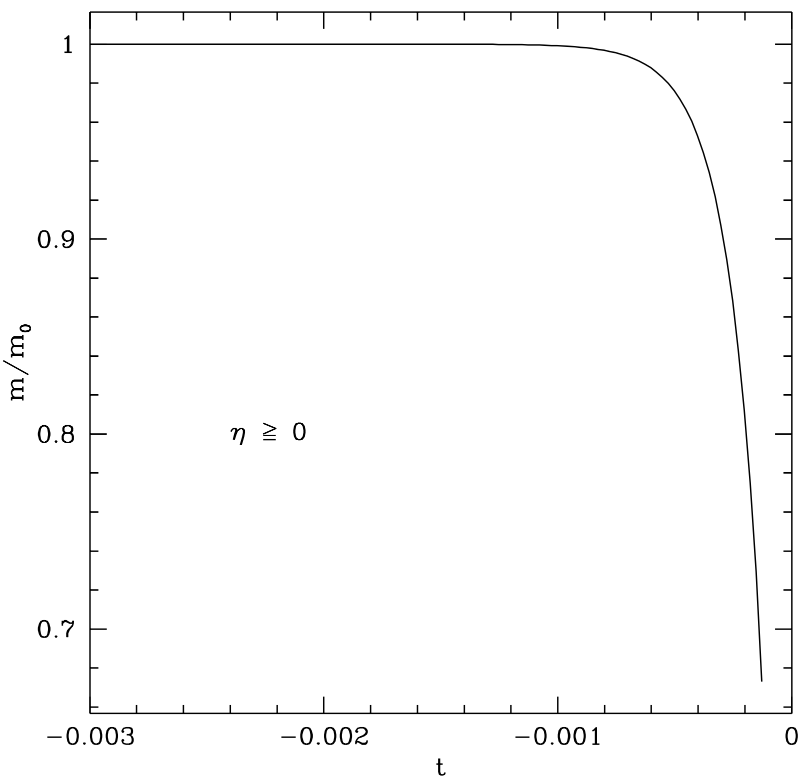

Figure 11. Time behaviour of the total energy entrapped inside the surface Σ for the models with and without shear viscosity. The time, m and m_0 are in units of seconds.

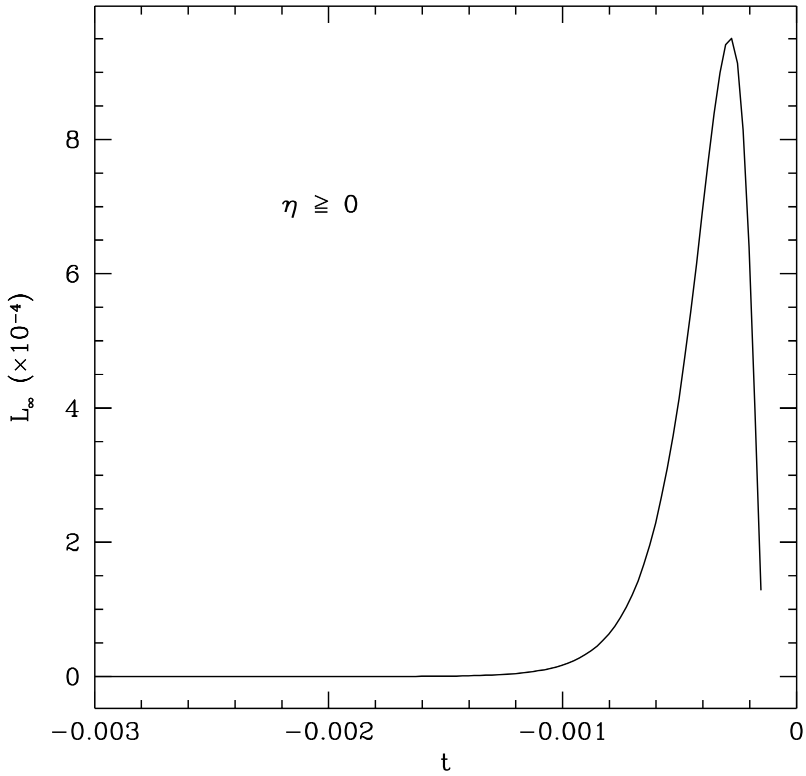

Figure 12. Time behaviour of the luminosity perceived by an observer at rest at infinity for the models with and without shear viscosity. The time is in units of second and the luminosity is dimensionless.

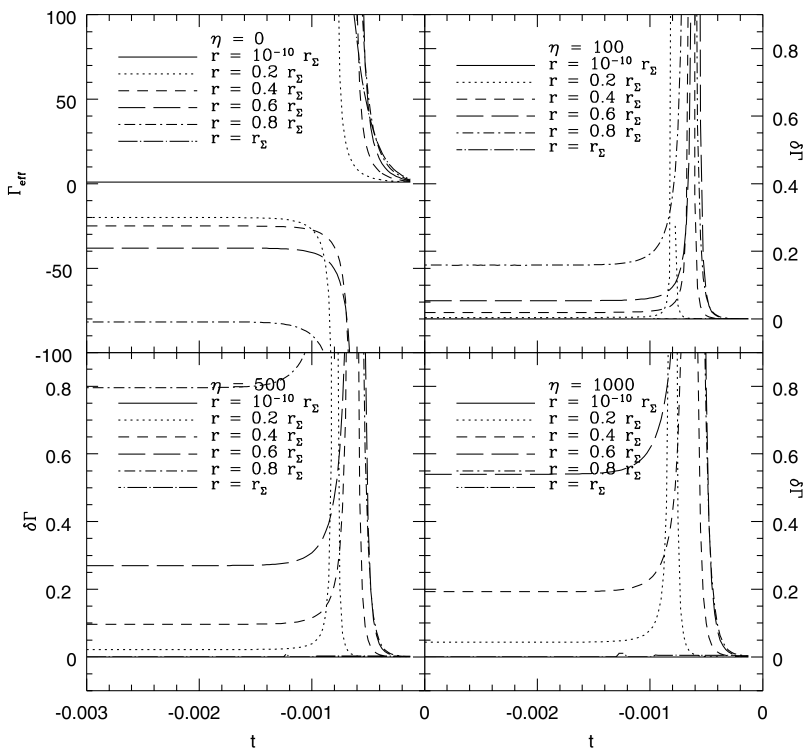

Figure 13. Time behaviour of the effective adiabatic index $\Gamma_{\rm eff}$ for four values of η. The quantity $\delta\Gamma$ is defined as $\Gamma_{\rm eff}(\eta \neq 0) - \Gamma_{\rm eff}(\eta = 0)$. The time is in units of seconds, $\Gamma_{\rm eff}$ and $\delta\Gamma$ are dimensionless.

$$d(r) = r_\Sigma^2 g^2(r), \tag{123}$$

$$e(r) = r_\Sigma^6 (r_\Sigma^2 - r^2) g(r), \tag{124}$$

$$h(r) = (1 + r^2)^2, \tag{125}$$

and

$$j(r) = 3a - 4\kappa\eta A_0. \tag{126}$$

Comparing the figures for $\Gamma_{\rm eff}$ ($\eta = 0$ and $\eta \neq 0$) we can see that the time evolution of the effective adiabatic indices are not very different graphically. This is the reason to plot the quantity $\delta\Gamma = \Gamma_{\rm eff}(\eta \neq 0) - \Gamma_{\rm eff}(\eta = 0)$ instead of $\Gamma_{\rm eff}$ for the $\eta \neq 0$ models. We can note in Fig. 13 ($\eta = 0$) that shortly before the peak of luminosity (see Fig. 12) there is a large discontinuity in $\Gamma_{\rm eff}$ owing mainly to the behaviour of the pressure. The effect of the viscosity is to increase much more these discontinuities.

Finally, models of radiating viscous spheres have been presented by Herrera et al. (1989). This work is particularly relevant for the proposed discussion because the conclusion concerning the effective adiabatic index is the same in both cases. Namely, a decreasing of the critical adiabatic index required for stability (Chan et al. 1994), or equivalently, an increasing of the effective adiabatic index, induced by viscosity. Since the models considered in each case are completely different, we suggest that this effect seems to be model independent.

8 CONCLUSIONS

The main conclusions of the present study are as follows.

(i) We have generalized the result which the pressure has non-zero value at the surface of the star unless the heat flux and shear viscosity vanish.

(ii) The pressure anisotropy increases with the shear viscosity.

(iii) The total radiated mass is equal for the non-viscous star and for the star with shear viscosity.

(iv) The star luminosity is the same for both collapsing models.

(v) The collapsing times with shear viscosity and without shear viscosity are the same.

(vi) The shear viscosity increases the value of the effective adiabatic index.

ACKNOWLEDGMENT

The author acknowledges financial support from the Brazilian CNPq.

REFERENCES

Arnett W. D., 1977, ApJ, 218, 815
Bonnor W. B., de Oliveira A. K. G., Santos N. O., 1989, Phys. Rep., 181, 269
Cahill M. E., McVittie G. C., 1970, J. Math. Phys., 11, 1382
Chan R., 1993, Ap&SS, 206, 219
Chan R., 1997, MNRAS, 288, 589
Chan R., 1998, MNRAS, 299, 811
Chan R., Herrera L., Santos N. O., 1994, MNRAS, 267, 637
Cutler C., Lindblom L., 1987, ApJ, 314, 234
de Oliveira A. K. G., Santos N. O., Kolassis C. A., 1985, MNRAS, 216, 1001
Herrera L., Santos N. O., 1997, Phys. Rep., 286, 53
Herrera L., Jiménez J., Barreto W., 1989, Can. J. Phys., 67, 855
Israel W., 1966a, Nuovo Cimento B, 44, 1
Israel W., 1966b, Nuovo Cimento B, 48, 463
Kazanas D., 1978, ApJ, 222, L109
Kolassis C. A., Santos N. O., Tsoubelis D., 1988, Class. Quantum Grav., 5, 1329
Martínez J., Pavón D., 1994, MNRAS, 268, 654
Raychaudhuri A. K., Maiti S. R., 1979, J. Math. Phys., 20, 245
Santos N. O., 1985, MNRAS, 216, 403
Vaidya P. C., 1953, Nat, 171, 260
Woosley S. E., Phillips M. M., 1988, Sci, 240, 750

This paper has been typeset from a TEX/LATEX file prepared by the author.